

## Supplementary Materials for

AutoTFCNNY: A Multi-Instance Neural Network for Enhanced Early

Cancer Detection Using TCR Data

DonghongYang<sup>1</sup>, XinPeng<sup>1</sup>, Yiming Zhou<sup>2</sup>, ShenglanPeng<sup>\*</sup>

<sup>1</sup> Jingdezhen Ceramic University, Jingdezhen, China

<sup>2</sup> Base and Byte Biotechnology Company Ltd, Beijing, China

<sup>\*</sup>Corresponding author. Email: \*solfix123@163.com

### **The PDF file includes:**

Fig. S1. ROC curve of AutoTFCNNY on 22 cancers, with confidence interval for the coefficient of 0.95.

Fig. S2. Sample characteristic difference heat map.

Fig. S3. Ablation experiment – number of PCA.

Fig. S4. Ablation experiment – Dropout.

Fig. S5. Ablation experiment– number of attentions.

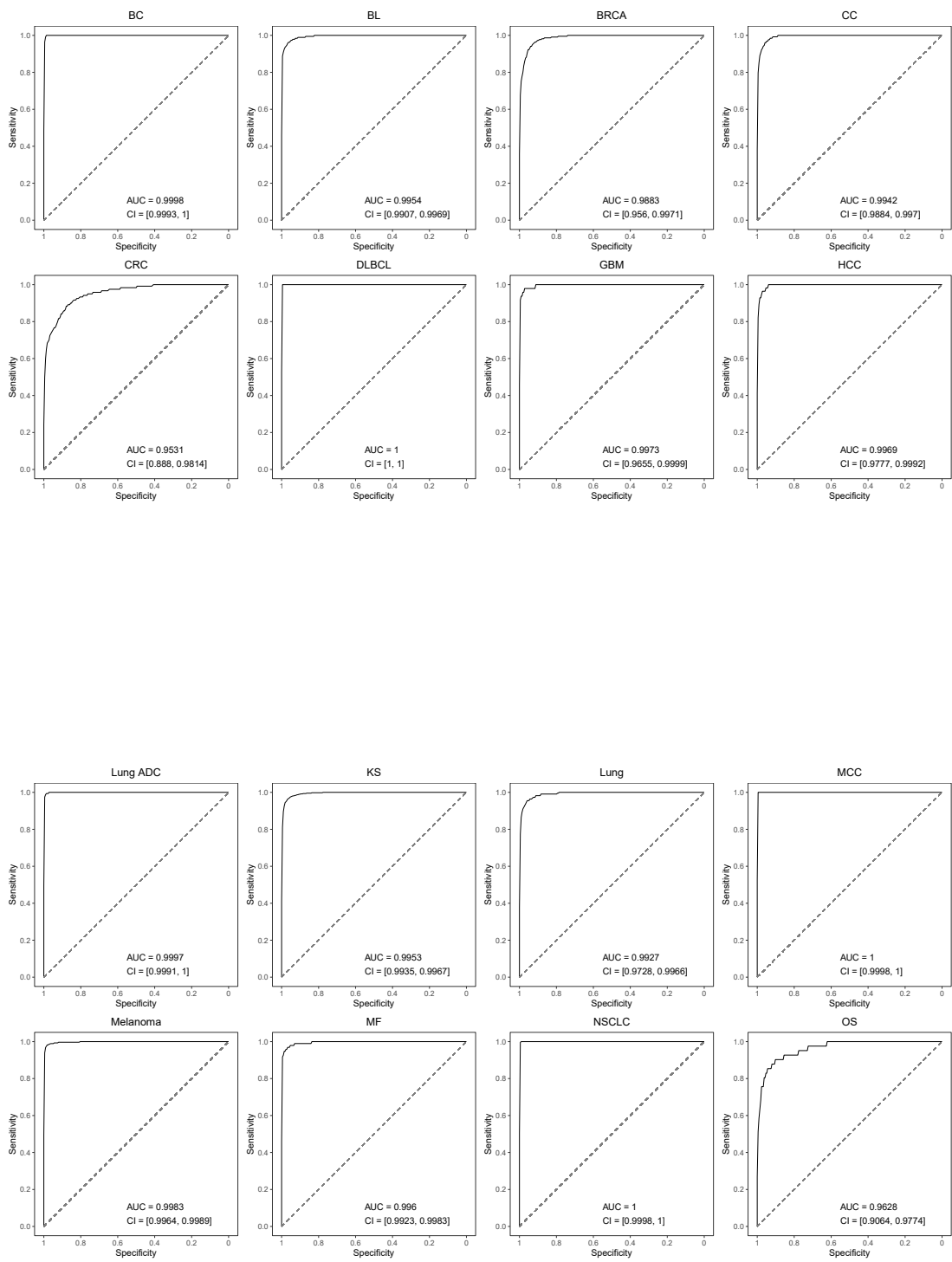
Fig. S6. Ablation experiment– number of encoders.

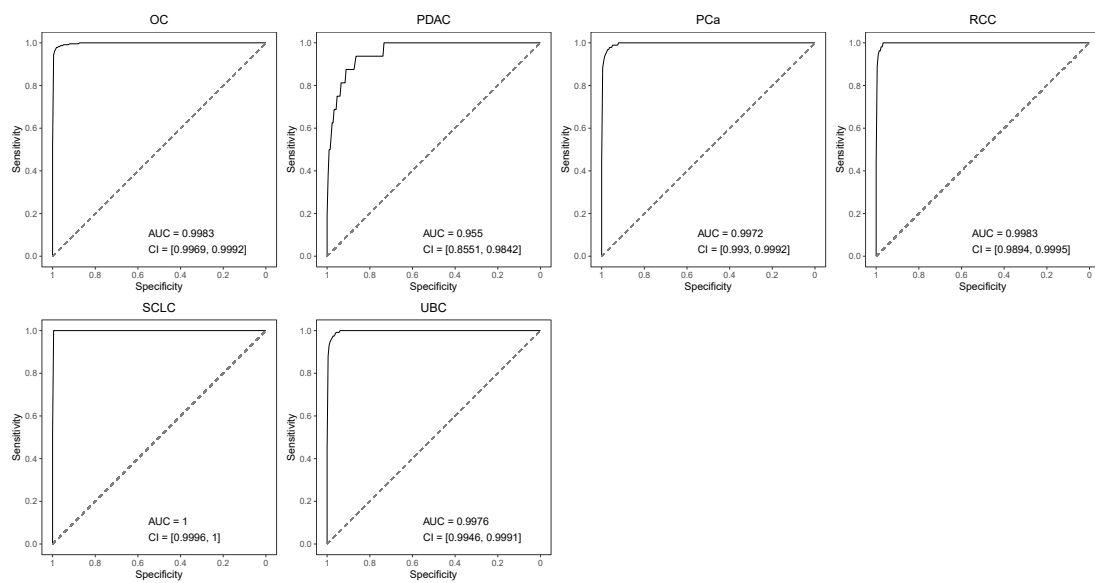
Table S1. Average performance of the models on the 22 cancer datasets.

Table S2. Summary information of experimental dataset.

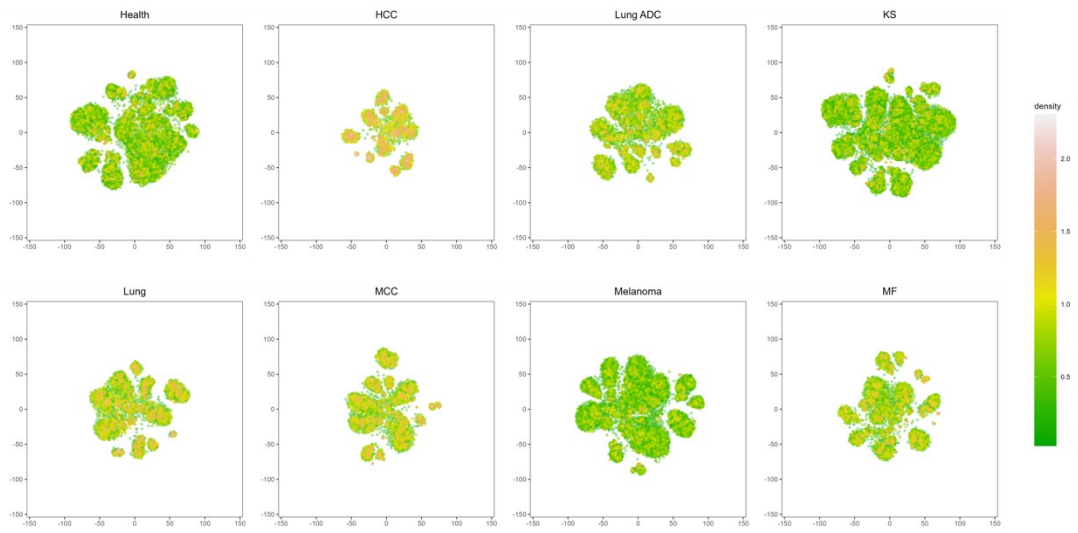
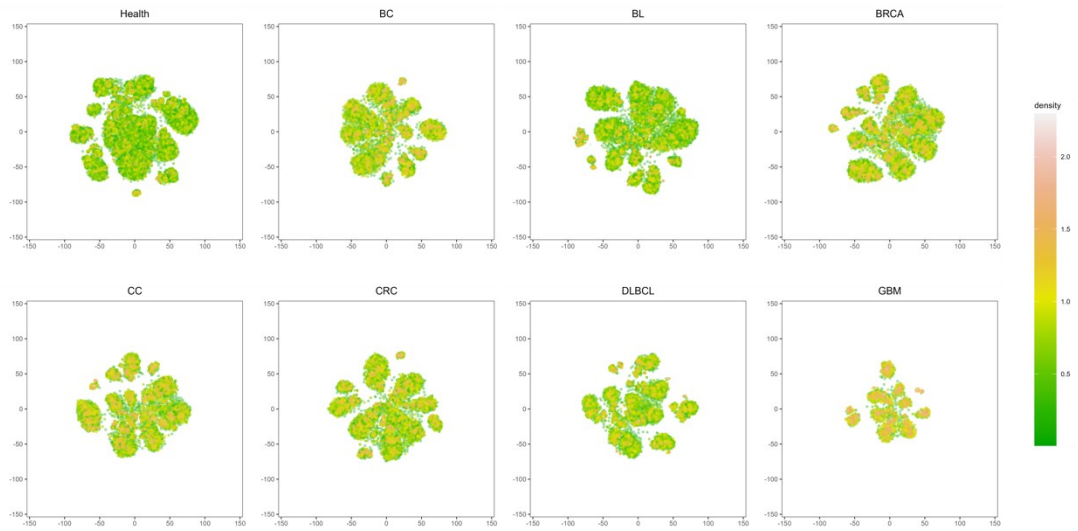
Table S3. Summary information of test datasets.







**Fig. S1. ROC curve of AutoTFCNNY on 22 cancers, with confidence interval for the coefficient of 0.95.**



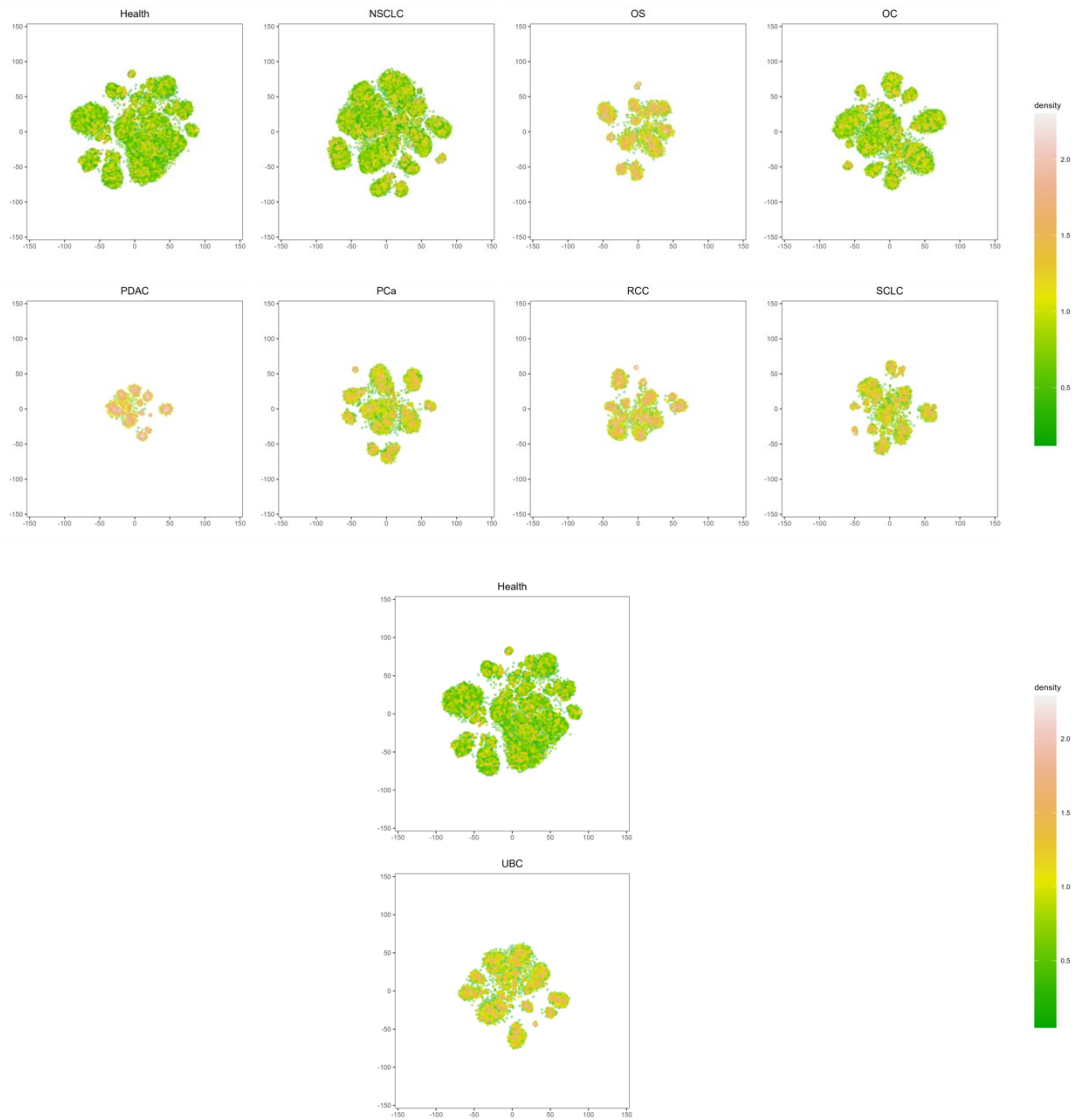


**Fig. S2. Sample characteristic difference heat map.** A pale yellow colour indicates a high density value, representing high-density regions of the TCR sequence. There is a higher concentration of TCR sequence points in these regions, which may indicate an increase in TCR sequence diversity in the cancer state. A green colour indicates a low density value, showing a lower density of TCR sequences. There are fewer TCR sequence points in these regions, which may reflect the stability of the TCR sequence in this state.

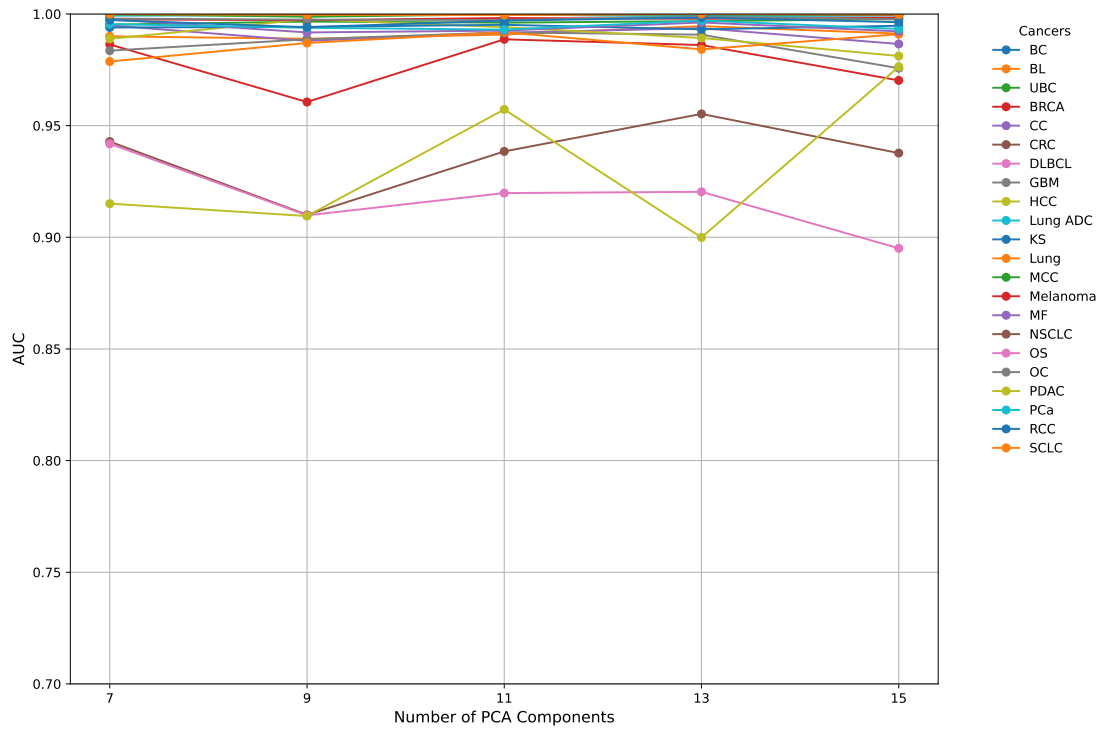


**Fig. S3. Ablation experiment – number of PCA.** This figure shows the impact of the first 7, 9, 11, 13 and 15 principal components on the model performance. The data are the 22 cancer datasets in this experiment, which are represented by lines of different colours in the figure. Each point represents the average AUC value of the 10 rounds of 5-fold cross-validation of the model with different numbers of principal components.

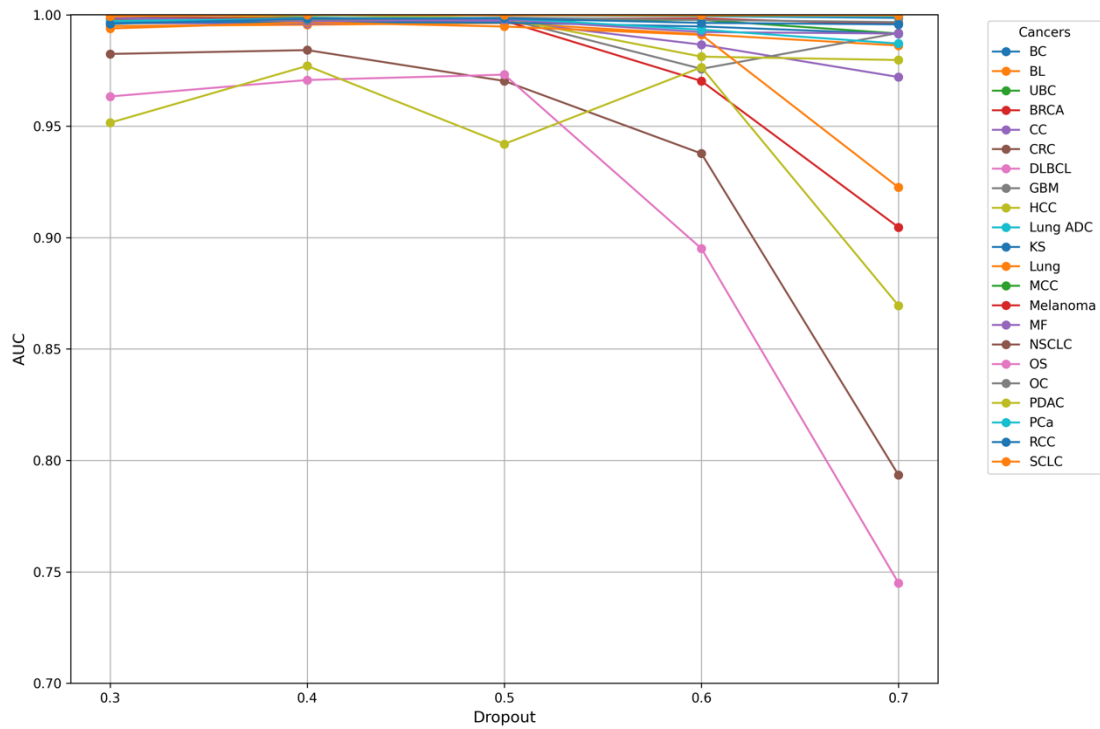


**Fig. S4. Ablation experiment – Dropout.** This graph shows the performance of the model as a function of the dropout value while holding other parameters constant. The data are the 22 cancer datasets in this experiment, which are represented by lines of different colours in the graph. Each point is the average AUC value of 10 rounds of 5-fold cross-validation of the model at different dropout values.

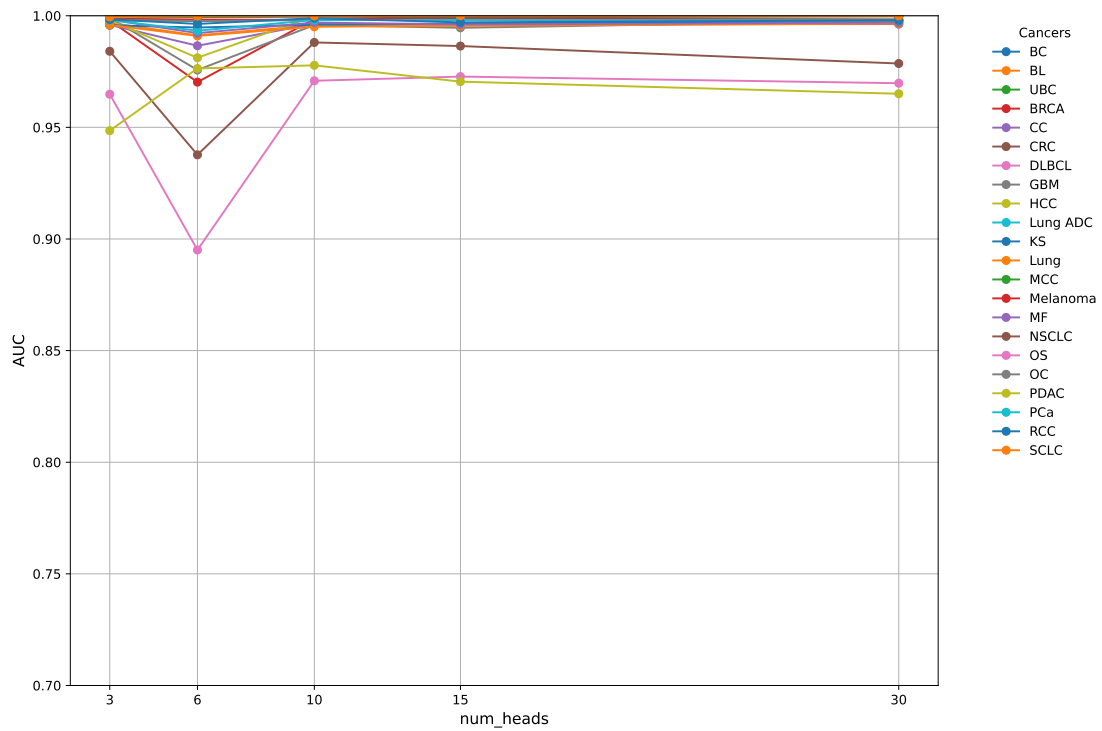


**Fig. S5. Ablation experiment– number of attentions.** This graph shows the performance of the model as a function of the number of attention heads while holding other parameters constant. The data are the 22 cancer datasets in this experiment, which are represented by lines of different colours in the graph. Each point represents the average AUC value of the 10-fold cross-validation of the model with different numbers of attention heads.

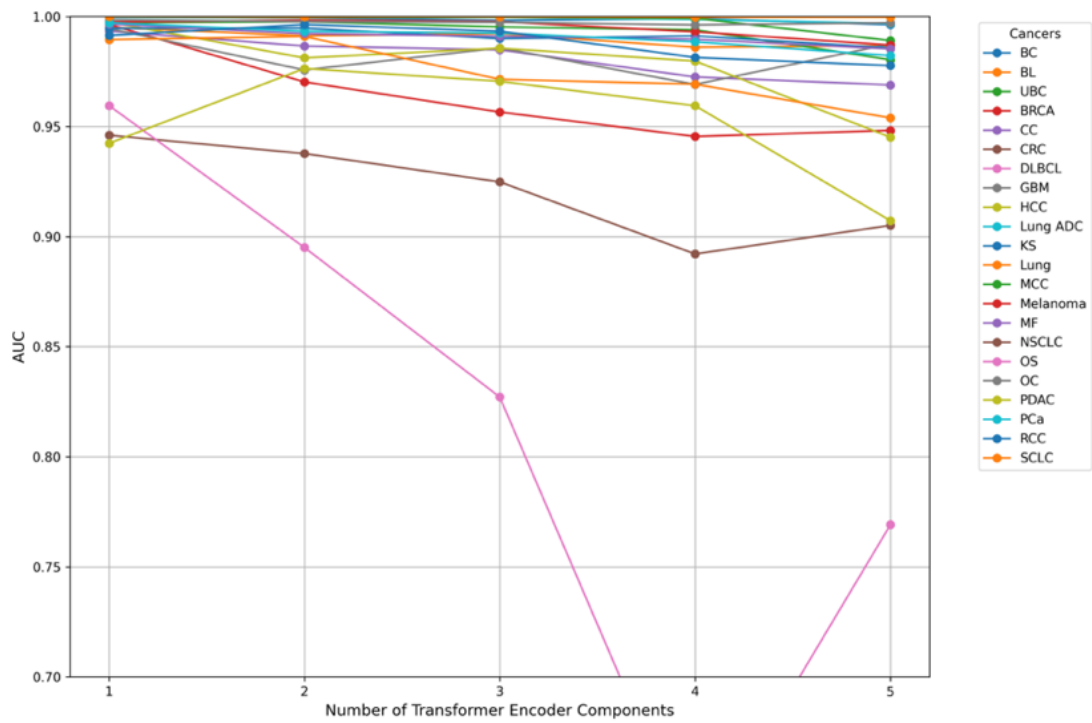


**Fig. S6. Ablation experiment– number of encoders.** This graph shows the performance of the model as a function of the number of encoders while holding other parameters constant. The data are the 22 cancer datasets in this experiment, represented by lines of different colours in the graph. Each point is the average AUC value of 10 rounds of 5-fold cross-validation for the model with different numbers of encoders.

## Supplementary Tables

**Table S1. Average performance of the models on the 22 cancer datasets.**

Types Cancer	Model	ACC		SEN		SPE		AUC	
BC	iCanTCR	0.976921	0.005654	0.966667	0.00727	0.982383	0.006993	0.993433	0.002725
	DeepLION	0.973049	0.008433	0.964737	0.016207	0.977477	0.008695	0.99669	0.001394
	DeepLION2	0.94003	0.041285	0.839825	0.119988	0.993411	0.006198	0.993467	0.007282
	MINN-SA	0.734725	0.054431	0.673932	0.122076	0.76711	0.070388	0.826799	0.060798
	TransMIL	0.775868	0.029072	0.55467	0.070319	0.893703	0.031548	0.828767	0.03469
	BiFormer	0.975335	0.004709	0.959474	0.012202	0.983785	0.005731	0.995431	0.001301
	AutoTFCNNY	0.990274	0.006245	0.996316	0.005015	0.987056	0.009599	<b>0.99971</b>	<b>0.000247</b>
BL	iCanTCR	0.954613	0.007393	0.943957	0.011836	0.963925	0.009875	0.986909	0.003828
	DeepLION	0.926334	0.020427	0.912193	0.024526	0.938692	0.02042	0.979262	0.008388
	DeepLION2	0.930374	0.020995	0.887914	0.042719	0.967477	0.026715	0.982598	0.008535
	MINN-SA	0.749969	0.039892	0.695781	0.099872	0.797319	0.068318	0.833838	0.040779
	TransMIL	0.742966	0.028043	0.681899	0.042047	0.796328	0.035924	0.818026	0.026257
	BiFormer	0.929526	0.007566	0.914225	0.011525	0.942897	0.010408	0.97812	0.003242
	AutoTFCNNY	0.959302	0.010018	0.957326	0.010025	0.961028	0.019994	<b>0.994948</b>	<b>0.001806</b>
BRCA	iCanTCR	0.955023	0.007911	0.963864	0.010223	0.945935	0.013583	<b>0.991234</b>	<b>0.002899</b>
	DeepLION	0.876336	0.056283	0.881227	0.061937	0.871308	0.059083	0.951857	0.033521
	DeepLION2	0.938203	0.032889	0.9605	0.021551	0.91528	0.069892	0.988165	0.008372
	MINN-SA	0.702649	0.05965	0.871304	0.049808	0.529265	0.141687	0.788794	0.059172
	TransMIL	0.704697	0.024451	0.714417	0.039301	0.694704	0.032744	0.768063	0.026205
	BiFormer	0.929885	0.007087	0.942773	0.010258	0.916636	0.011987	0.979484	0.003079
	AutoTFCNNY	0.90841	0.039392	0.981955	0.032001	0.832804	0.070109	0.985651	0.013108
CC	iCanTCR	0.94652	0.007105	0.938359	0.015856	0.951402	0.010353	0.981747	0.003895
	DeepLION	0.89693	0.027806	0.843594	0.047215	0.928832	0.022345	0.959941	0.016221
	DeepLION2	0.90345	0.038321	0.780703	0.104393	0.976869	0.01365	0.974397	0.015467
	MINN-SA	0.782887	0.037527	0.653488	0.128083	0.860285	0.04617	0.853912	0.044179
	TransMIL	0.718944	0.028257	0.482165	0.071959	0.860568	0.031437	0.761838	0.039334
	BiFormer	0.91386	0.009408	0.865234	0.018055	0.942944	0.01104	0.968807	0.003758
	AutoTFCNNY	0.956959	0.01355	0.946484	0.022956	0.963224	0.019665	<b>0.994024</b>	<b>0.00271</b>
CRC	iCanTCR	0.942036	0.00982	0.91	0.018196	0.96	0.011356	<b>0.977921</b>	<b>0.005329</b>

	DeepLION	0.83015	0.028962	0.725583	0.056149	0.888785	0.020728	0.9031	0.027436
	DeepLION2	0.880419	0.030654	0.735833	0.090798	0.961495	0.02354	0.953512	0.016889
	MINN-SA	0.677312	0.046563	0.492088	0.115036	0.781176	0.109418	0.707248	0.047368
	TransMIL	0.691617	0.02682	0.364815	0.076047	0.87487	0.035409	0.708677	0.037861
	BiFormer	0.89012	0.013182	0.828917	0.027764	0.924439	0.015844	0.95322	0.007282
	AutoTFCNNY	0.856707	0.049791	0.869333	0.096748	0.849626	0.081202	0.948664	0.026823
DLBCL	iCanTCR	0.990556	0.005253	0.977609	0.012909	0.996121	0.003988	0.998698	0.001823
	DeepLION	0.99402	0.0036	0.982283	0.011422	0.999065	0.002203	0.999846	0.000281
	DeepLION2	0.944641	0.033404	0.81663	0.111809	0.999673	0.003271	0.999416	0.001069
	MINN-SA	0.922559	0.021171	0.814119	0.076946	0.969178	0.008804	0.96853	0.014501
	TransMIL	0.847792	0.021992	0.648112	0.063124	0.933635	0.020115	0.900772	0.025203
	BiFormer	0.99415	0.002985	0.981087	0.010086	0.999766	0.001024	0.999956	0.000073
AutoTFCNNY	0.999771	0.000838	0.999239	0.002787	1	0	1	0	
GBM	iCanTCR	0.956183	0.009742	0.843958	0.053832	0.981355	0.009567	0.983398	0.0089
	DeepLION	0.949313	0.014395	0.783542	0.069248	0.986495	0.007363	0.982869	0.009043
	DeepLION2	0.914084	0.020207	0.53125	0.110458	0.999953	0.000467	0.985333	0.016138
	MINN-SA	0.852456	0.017837	0.246212	0.116618	0.988436	0.01237	0.751443	0.085423
	TransMIL	0.835801	0.017104	0.302189	0.084146	0.955489	0.014431	0.761747	0.043987
	BiFormer	0.973511	0.006901	0.92	0.031158	0.985514	0.006457	<b>0.995438</b>	<b>0.00184</b>
AutoTFCNNY	0.971565	0.0276	0.913542	0.076037	0.984579	0.02786	0.9923	0.011265	
HCC	iCanTCR	0.925444	0.013724	0.803571	0.051204	0.957336	0.0118	0.970411	0.010378
	DeepLION	0.920407	0.01963	0.744286	0.080857	0.966495	0.009964	0.962926	0.018817
	DeepLION2	0.919222	0.015172	0.618393	0.0742	0.997944	0.004617	0.988019	0.010116
	MINN-SA	0.794126	0.009568	0.052128	0.051634	0.988294	0.01457	0.636972	0.069503
	TransMIL	0.830228	0.021195	0.39899	0.077928	0.943076	0.021809	0.748404	0.042129
	BiFormer	0.934037	0.0099	0.793036	0.040139	0.970935	0.007705	0.979302	0.004104
AutoTFCNNY	0.96463	0.021033	0.928036	0.069576	0.974206	0.023213	<b>0.993783</b>	<b>0.008922</b>	
KS	iCanTCR	0.962318	0.006123	0.973898	0.006097	0.936776	0.015696	0.992607	0.002035
	DeepLION	0.935496	0.009963	0.966949	0.008103	0.866121	0.02754	0.97891	0.004658
	DeepLION2	0.93188	0.017193	0.984661	0.00666	0.815467	0.056761	0.98514	0.005984
	MINN-SA	0.75737	0.020502	0.896037	0.029834	0.451525	0.090149	0.787147	0.027035
	TransMIL	0.747769	0.019209	0.897342	0.021053	0.41787	0.054691	0.769145	0.026709

	BiFormer	0.932536	0.007039	0.962669	0.006637	0.866075	0.017738	0.976441	0.003805
	AutoTFCNNY	0.965364	0.00638	0.986631	0.005018	0.918458	0.021536	<b>0.995308</b>	<b>0.001112</b>
Lung	iCanTCR	0.937877	0.010197	0.88964	0.020543	0.962897	0.010498	0.979515	0.0054
	DeepLION	0.903938	0.021248	0.834865	0.049643	0.939766	0.015404	0.963606	0.014317
	DeepLION2	0.921446	0.030727	0.802072	0.092987	0.983364	0.01116	0.978812	0.010689
	MINN-SA	0.65296	0.069949	0.566294	0.126735	0.697914	0.108396	0.695223	0.087395
	TransMIL	0.739052	0.025892	0.491491	0.067359	0.86746	0.030243	0.757057	0.034992
	BiFormer	0.923015	0.009818	0.868018	0.023554	0.951542	0.009754	0.978922	0.003761
	AutoTFCNNY	0.942369	0.030296	0.941441	0.0518	0.94285	0.043263	<b>0.990132</b>	<b>0.007699</b>
Lung ADC	iCanTCR	0.985618	0.004032	0.988165	0.005665	0.983738	0.005536	0.998883	0.000612
	DeepLION	0.969892	0.023099	0.973671	0.028071	0.967103	0.022853	0.995809	0.006594
	DeepLION2	0.978575	0.011522	0.972215	0.025042	0.983271	0.009183	0.998151	0.001632
	MINN-SA	0.791273	0.038415	0.721263	0.106495	0.842962	0.039969	0.875815	0.032841
	TransMIL	0.78405	0.025978	0.722606	0.041798	0.829416	0.031477	0.849089	0.027484
	BiFormer	0.977446	0.004535	0.985759	0.007706	0.971308	0.006576	0.997332	0.000874
	AutoTFCNNY	0.983468	0.010494	0.995506	0.005191	0.974579	0.018132	<b>0.999621</b>	<b>0.000362</b>
MCC	iCanTCR	0.988951	0.005346	0.979722	0.014828	0.992056	0.004812	0.998709	0.001193
	DeepLION	0.981783	0.007941	0.957083	0.021902	0.990093	0.006911	0.998168	0.001409
	DeepLION2	0.945594	0.030394	0.788333	0.118972	0.998505	0.006834	0.998124	0.005281
	MINN-SA	0.839797	0.021895	0.510662	0.110682	0.950533	0.017999	0.875616	0.040165
	TransMIL	0.800381	0.025015	0.371352	0.085354	0.944728	0.023096	0.795586	0.045402
	BiFormer	0.986294	0.006826	0.98125	0.015339	0.987991	0.007068	0.999173	0.000778
	AutoTFCNNY	0.996189	0.00419	0.99625	0.006197	0.996168	0.005492	<b>0.999952</b>	<b>0.000091</b>
MF	iCanTCR	0.949968	0.008473	0.911979	0.021475	0.967009	0.009735	0.984308	0.00622
	DeepLION	0.956355	0.009446	0.908646	0.021903	0.977757	0.007973	0.988909	0.003475
	DeepLION2	0.906097	0.034317	0.704792	0.114284	0.996402	0.007149	0.98508	0.007199
	MINN-SA	0.827142	0.026906	0.612269	0.104851	0.923534	0.024368	0.884574	0.029112
	TransMIL	0.771522	0.025642	0.44455	0.077321	0.918201	0.024549	0.802808	0.038572
	BiFormer	0.963484	0.005905	0.921771	0.011029	0.982196	0.006565	0.987092	0.002606
	AutoTFCNNY	0.971129	0.006259	0.915937	0.018566	0.995888	0.005839	<b>0.995937</b>	<b>0.001804</b>
Melanoma	iCanTCR	0.958323	0.007067	0.967046	0.008623	0.946869	0.015571	0.993631	0.001905
	DeepLION	0.945434	0.011562	0.950712	0.0129	0.938505	0.014862	0.988294	0.003822

	DeepLION2	0.953636	0.016312	0.966833	0.015614	0.936308	0.038726	0.992386	0.003088
	MINN-SA	0.74927	0.060141	0.922032	0.03783	0.52242	0.156781	0.842883	0.062288
	TransMIL	0.767105	0.027965	0.814336	0.030912	0.705088	0.041388	0.841306	0.027121
	BiFormer	0.940545	0.006643	0.954698	0.007345	0.921963	0.013876	0.986392	0.002656
	AutoTFCNNY	0.975879	0.007481	0.988399	0.004485	0.959439	0.015869	<b>0.998096</b>	<b>0.000773</b>
NSCLC	iCanTCR	0.980137	0.006842	0.984107	0.005543	0.975981	0.012759	0.995488	0.002611
	DeepLION	0.984726	0.005388	0.985759	0.007198	0.983645	0.008202	0.999117	0.000473
	DeepLION2	0.962785	0.035629	0.969509	0.040862	0.955748	0.05126	0.994628	0.010261
	MINN-SA	0.883077	0.037131	0.912653	0.044438	0.852119	0.056346	0.960191	0.021011
	TransMIL	0.80619	0.031848	0.818317	0.038129	0.793496	0.038172	0.887424	0.030273
	BiFormer	0.978402	0.003663	0.980446	0.006079	0.976262	0.006359	0.998303	0.000517
	AutoTFCNNY	0.994018	0.003023	0.998571	0.002187	0.989252	0.006141	<b>0.999929</b>	<b>0.000122</b>
OC	iCanTCR	0.954437	0.007735	0.954652	0.012098	0.954206	0.016119	0.988358	0.00322
	DeepLION	0.949077	0.023478	0.953348	0.022763	0.944486	0.02836	0.990771	0.008284
	DeepLION2	0.9375	0.0438	0.947174	0.042372	0.927103	0.08019	0.9871	0.016085
	MINN-SA	0.771726	0.045883	0.894862	0.046086	0.639384	0.098145	0.865436	0.039784
	TransMIL	0.765152	0.027017	0.76043	0.034841	0.770226	0.036934	0.843796	0.025298
	BiFormer	0.948649	0.005894	0.941826	0.009347	0.955981	0.011603	0.990887	0.001891
	AutoTFCNNY	0.974369	0.007164	0.984043	0.005699	0.963972	0.015004	<b>0.998194</b>	<b>0.000782</b>
OS	iCanTCR	0.943059	0.0107	0.803415	0.061705	0.969813	0.006522	<b>0.953319</b>	<b>0.012294</b>
	DeepLION	0.869412	0.014379	0.288537	0.086323	0.980701	0.008651	0.835986	0.045572
	DeepLION2	0.87051	0.010277	0.195122	0.064484	0.999907	0.000658	0.925323	0.032737
	MINN-SA	0.861596	0.00872	0.183543	0.060183	0.991504	0.007045	0.715094	0.080271
	TransMIL	0.83775	0.009533	0.044592	0.041672	0.98971	0.010341	0.66112	0.051742
	BiFormer	0.910078	0.010711	0.606585	0.050554	0.968224	0.009486	0.912717	0.011602
	AutoTFCNNY	0.93149	0.029013	0.701951	0.098088	0.975467	0.031855	0.952545	0.02974
PCa	iCanTCR	0.941883	0.010768	0.907872	0.035468	0.956822	0.016896	0.984323	0.004284
	DeepLION	0.927825	0.017111	0.864681	0.035107	0.955561	0.014844	0.978568	0.008722
	DeepLION2	0.822792	0.047834	0.440957	0.164984	0.990514	0.010406	0.930232	0.043495
	MINN-SA	0.75856	0.031157	0.337847	0.131282	0.943359	0.035313	0.778543	0.073159
	TransMIL	0.765479	0.021887	0.472276	0.056698	0.89427	0.026422	0.784345	0.030659
	BiFormer	0.933247	0.007446	0.895426	0.017766	0.94986	0.008424	0.980372	0.003751

	AutoTFCNNY	0.97276	0.010245	0.946277	0.025633	0.984393	0.009811	<b>0.996686</b>	<b>0.002799</b>
PDAC	iCanTCR	0.921217	0.01145	0.121875	0.067872	0.980981	0.01428	0.75446	0.071125
	DeepLION	0.93113	0.00348	0.0225	0.040241	0.999065	0.002301	0.789355	0.052129
	DeepLION2	0.930478	0.000435	0.000625	0.00625	1	0	0.771043	0.082504
	MINN-SA	0.930435	0	0	0	1	0	0.47994	0.050361
	TransMIL	0.922354	0.010989	0.087753	0.068535	0.984754	0.010961	0.514154	0.08095
	BiFormer	0.940739	0.007303	0.23125	0.109341	0.993785	0.005274	0.853645	0.060145
	AutoTFCNNY	0.946478	0.010167	0.261875	0.145344	0.997664	0.004279	<b>0.94965</b>	<b>0.033732</b>
RCC	iCanTCR	0.948202	0.012799	0.877736	0.044753	0.965654	0.012626	0.974588	0.011604
	DeepLION	0.94397	0.01208	0.792453	0.056253	0.981495	0.006803	0.973557	0.011453
	DeepLION2	0.914082	0.020997	0.568113	0.106831	0.999766	0.001922	0.987377	0.011608
	MINN-SA	0.839973	0.023346	0.26701	0.149161	0.981875	0.01312	0.79351	0.083712
	TransMIL	0.847312	0.018487	0.390128	0.086498	0.96054	0.018454	0.792349	0.037457
	BiFormer	0.949775	0.010199	0.831321	0.048481	0.979112	0.006657	0.978774	0.006761
	AutoTFCNNY	0.975918	0.010174	0.905283	0.042739	0.993411	0.007125	<b>0.997364</b>	<b>0.00398</b>
SCLC	iCanTCR	0.984887	0.004867	0.951346	0.022449	0.993037	0.00443	0.993839	0.004481
	DeepLION	0.975639	0.009932	0.899615	0.044292	0.994112	0.004998	0.996756	0.002537
	DeepLION2	0.918383	0.027132	0.583846	0.138554	0.999673	0.001198	0.994047	0.01396
	MINN-SA	0.866105	0.022701	0.422883	0.132453	0.973803	0.01275	0.860526	0.068082
	TransMIL	0.833333	0.018093	0.315657	0.083102	0.959124	0.017565	0.791513	0.047462
	BiFormer	0.983872	0.005077	0.949615	0.02131	0.992196	0.003932	0.997918	0.001142
	AutoTFCNNY	0.99688	0.004781	0.993269	0.01456	0.997757	0.004625	<b>0.999933</b>	<b>0.0002</b>
UBC	iCanTCR	0.953293	0.00896	0.932735	0.01784	0.964533	0.01288	0.9878	0.00409
	DeepLION	0.913988	0.025651	0.857863	0.054905	0.944673	0.018222	0.972939	0.014348
	DeepLION2	0.930544	0.030877	0.83	0.090322	0.985514	0.011964	0.986713	0.008951
	MINN-SA	0.72236	0.046421	0.533886	0.165622	0.825404	0.074493	0.769264	0.072773
	TransMIL	0.776343	0.023939	0.608996	0.054445	0.867837	0.028837	0.818024	0.029568
	BiFormer	0.942054	0.009372	0.924188	0.020782	0.951822	0.010347	0.985136	0.003949
	AutoTFCNNY	0.972024	0.011145	0.943675	0.030421	0.987523	0.009323	<b>0.997517</b>	<b>0.001447</b>

The maximum AUC values for the evaluation metrics in the comparison models are shown in bold. The values in parentheses represent standard deviations. BC: Brain Cancer; BL: Burkitt Lymphoma; BRCA: Breast Cancer; CC: Cervical Cancer ; CRC: Colorectal Cancer; DLBCL: Lymphoid Neoplasm Diffuse Large B-cell Lymphoma; GBM: Glioblastoma Multiforme; HCC: Hepatocellular Carcinoma;

KS: Kaposi sarcoma; Lung: Lung Cancer; Lung ADC: Lung Adenocarcinomas; MCC: Merkel Cell Carcinoma; MF: Mycosis fungoides; Melanoma; NSCLC: Non-small Cell Lung Cancer; OC: Ovarian Cancer; OS: Osteosarcoma; PCa: Prostate Cancer; PDAC: Pancreatic Ductal Adenocarcinoma; RCC: Renal Cell Carcinoma; SCLC: Small-cell Lung Cancer; UBC: Urothelial Bladder Cancer; ACC, accuracy; SEN, sensitivity; SPE, specificity; AUC, area under the receiver operating characteristic curve.

**Table S2. Summary information of experimental dataset.**

Disease	Total sample size	Sample size	Data type	LOCUS	Study	immuneACCESS DOI or DOI
<b>BC</b>	114	144	TCR -seq	TCRB	Kudo Y et al.	<a href="https://doi.org/10.21417/YK2019AO">https://doi.org/10.21417/YK2019AO</a>
<b>BL</b>	187	153	TCR -seq	IGKLIGHTCR B	K Lombardo et al.,	<a href="https://doi.org/10.21417/B7MS37">https://doi.org/10.21417/B7MS37</a>
		115	TCR -seq	TCRB	J Rieken et al.	<a href="https://doi.org/10.21417/JR20202BJH">https://doi.org/10.21417/JR20202BJH</a>
<b>BRCA</b>	220	115	TCR -seq	TCRB	DB Page et al.	<a href="https://doi.org/10.21417/DBP2016CIR">https://doi.org/10.21417/DBP2016CIR</a>
		107	TCR -seq	TCRB	Page DB et al.	<a href="https://doi.org/10.21417/DBP2023NPJ">https://doi.org/10.21417/DBP2023NPJ</a>
<b>CC</b>	128	128	TCR -seq	TCRB	L Colbert et al.	<a href="https://doi.org/10.21417/LC2023CC">https://doi.org/10.21417/LC2023CC</a>
<b>CRC</b>	120	92	TCR -seq	TCRB	Høye E et al.	<a href="https://doi.org/10.21417/EH2023GS">https://doi.org/10.21417/EH2023GS</a>
		28	TCR -seq	TCRB	AM Sherwood et al.	<a href="https://doi.org/10.21417/B7PP46">https://doi.org/10.21417/B7PP46</a>
<b>DLBCL</b>	92	92	TCR -seq	TCRB	C Keane et al.	<a href="https://doi.org/10.21417/B7C301">https://doi.org/10.21417/B7C301</a>
<b>GBM</b>	48	48	TCR -seq	TCRB	MS Hsu et al.	<a href="https://doi.org/10.21417/B7D59F">https://doi.org/10.21417/B7D59F</a>
<b>HCC</b>	56	56	TCR -seq	TCRB	M Yarchoan et al.	<a href="https://doi.org/10.21417/RP2024NM">https://doi.org/10.21417/RP2024NM</a>
<b>KS</b>	472	474	TCR -seq	TCRB	S Ravishankar et al.	<a href="https://doi.org/10.21417/SR2024JEM">https://doi.org/10.21417/SR2024JEM</a>

<b>Lung</b>	111	40	TCR -seq	TCRB	AS Mansfield et al.	<a href="https://doi.org/10.21417/B71P7F">https://doi.org/10.21417/B71P7F</a>
		29	TCR -seq	TCRB	JX Caushi et al.	<a href="https://doi.org/10.21417/JC2021N">https://doi.org/10.21417/JC2021N</a>
		22	TCR -seq	TCRB	D Hamm	<a href="https://doi.org/10.21417/ADPT2020V4C">https://doi.org/10.21417/ADPT2020V4C</a> <a href="#">D</a>
		20	TCR -seq	TCRB	SC Formenti et al.	<a href="https://doi.org/10.21417/B7BW6X">https://doi.org/10.21417/B7BW6X</a>
<b>Lung ADC</b>	158	158	TCR -seq	TCRB	H. Dejima et al.	<a href="https://doi.org/10.1038/s41467-021-22890-x">https://doi.org/10.1038/s41467-021-22890-x</a>
<b>MCC</b>	72	72	TCR -seq	TCRB	M Farah et al.	<a href="https://doi.org/10.21417/MF2020JID">https://doi.org/10.21417/MF2020JID</a>
<b>MF</b>	96	68	TCR -seq	TCRB	D. Joffe et al.	<a href="https://doi.org/10.21417/DJ2023BA">https://doi.org/10.21417/DJ2023BA</a>
		28	TCR -seq	TCRB	Z Yu et al.	<a href="https://doi.org/10.21417/RC2023JID">https://doi.org/10.21417/RC2023JID</a>
<b>Melanoma</b>	281	199	TCR -seq	TCRB	W Pruessmann et al.	<a href="https://doi.org/10.21417/WP2019NC">https://doi.org/10.21417/WP2019NC</a>
		84	TCR -seq	TCRB	Huhtanen J et al.	<a href="https://doi.org/10.21417/JH2023JCI">https://doi.org/10.21417/JH2023JCI</a>
<b>NSCLC</b>	224	224	TCR -seq	TCRB	A Reuben et al.	<a href="https://doi.org/10.21417/AR2019NC">https://doi.org/10.21417/AR2019NC</a>
<b>OC</b>	230	96	TCR -seq	TCRB	Ryan O Emerson et al.	<a href="https://doi.org/10.21417/B7TG64">https://doi.org/10.21417/B7TG64</a>
		90	TCR -seq	TCRB	s Lee; L Zhao et al.	<a href="https://doi.org/10.21417/LS2021iS">https://doi.org/10.21417/LS2021iS</a>
		44	TCR -seq	TCRB	K Yoshida-Court et al.	<a href="https://doi.org/10.21417/KC2023PO">https://doi.org/10.21417/KC2023PO</a>
<b>OS</b>	41	41	TCR -seq	TCRB	C Wu et al.	<a href="https://doi.org/10.21417/CW2020NC">https://doi.org/10.21417/CW2020NC</a>
<b>PCa</b>	94	94	TCR -seq	TCRB	E Shenderov et al.	<a href="https://doi.org/10.21417/ES2023NM">https://doi.org/10.21417/ES2023NM</a>
<b>PDAC</b>	16	16	TCR -seq	TCRB	Stromnes I et al.	<a href="https://doi.org/10.21417/B7305D">https://doi.org/10.21417/B7305D</a>
<b>RCC</b>	53	53	TCR -seq	TCRB	J Chow et al.	<a href="https://doi.org/10.21417/JC2020PNAS">https://doi.org/10.21417/JC2020PNAS</a>
<b>SCLC</b>	52	52	TCR -seq	TCRB	M Chen et al.	<a href="https://doi.org/10.21417/MC2021NC">https://doi.org/10.21417/MC2021NC</a>
<b>UBC</b>	117	117	TCR -seq	TCRB	A Snyder et al.	<a href="https://doi.org/10.21417/B7MG68">https://doi.org/10.21417/B7MG68</a>
<b>Health</b>	214	214	TCR -seq	TCRB	Ying Xu et al.	<a href="https://doi.org/10.3389/fgene.2022.860510">https://doi.org/10.3389/fgene.2022.860510</a>

BC: Brain Cancer; BL: Burkitt Lymphoma; BRCA: Breast Cancer; CC: Cervical Cancer ; CRC: Colorectal Cancer; DLBCL: Lymphoid Neoplasm Diffuse Large B-cell Lymphoma; GBM: Glioblastoma Multiforme; HCC: Hepatocellular Carcinoma; KS: Kaposi sarcoma; Lung: Lung Cancer; Lung ADC: Lung Adenocarcinomas; MCC: Merkel Cell Carcinoma; MF: Mycosis fungoides; Melanoma; NSCLC: Non-small Cell Lung Cancer; OC: Ovarian Cancer; OS: Osteosarcoma; PCa: Prostate Cancer; PDAC: Pancreatic Ductal Adenocarcinoma; RCC: Renal Cell Carcinoma; SCLC: Small-cell Lung Cancer; UBC: Urothelial Bladder Cancer; Health: Non-cancer; T Cell Receptor-sequencing.

**Table S3. Summary information of test datasets.**

Disease	Sample size	Data type	LOCUS	Study	immuneACCESS DOI or DOI
UBC	12	TCR-seq	TCRB	Sankin A et al.	<a href="https://doi.org/10.21417/AS2019UO">https://doi.org/10.21417/AS2019UO</a>
BRCA	23	TCR-seq	TCRB	Muraro E et al.	<a href="https://doi.org/10.21417/EM2022FO">https://doi.org/10.21417/EM2022FO</a>
NSCLC	66	TCR-seq	TCRB	Kargl J et al.	<a href="https://doi.org/10.21417/B7B88G">https://doi.org/10.21417/B7B88G</a>
Melanoma	21	TCR-seq	TCRB	Huhtanen J - et al.	<a href="https://doi.org/10.21417/JH2022NC">https://doi.org/10.21417/JH2022NC</a>
CRC	10	TCR-seq	TCRB	Rajamanickam V et al.	<a href="https://doi.org/10.21417/vr2021cir">https://doi.org/10.21417/vr2021cir</a>
Health	51	TCR-seq	TCRB	Ying Xu et al.	<a href="https://doi.org/10.3389/fgene.2022.860510">https://doi.org/10.3389/fgene.2022.860510</a>

BRCA: Breast Cancer; CRC: Colorectal Cancer; Melanoma; NSCLC: Non-small Cell Lung Cancer; UBC: Urothelial Bladder Cancer; TCR-seq: Health: Non-cancer; T Cell Receptor-sequencing.